ARTICLE

Insight on Fractal Assessment Strategies for Tin Dioxide Thin Films

Zhiwen Chen,[†,‡,*] Dengyu Pan,[†] Bing Zhao,[†] Guoji Ding,[†] Zheng Jiao,[†] Minghong Wu,[†,*] Chan-Hung Shek,[‡] Lawrence C. M. Wu,[‡] and Joseph K. L. Lai[‡]

[†]School of Environmental and Chemical Engineering, Shanghai University, Shanghai 200444, People's Republic of China, and [‡]Department of Physics and Materials Science, City University of Hong Kong, Tat Chee Avenue, Kowloon Tong, Hong Kong

ABSTRACT Tin oxide is a unique material of widespread technological applications, particularly in the field of environmental functional materials. New strategies of fractal assessment for tin dioxide thin films formed at different substrate temperatures are of fundamental importance in the development of microdevices, such as gas sensors for the detection of environmental pollutants. Here, tin dioxide thin films with interesting fractal features were successfully prepared by pulsed laser deposition techniques under different substrate temperatures. Fractal method has been first applied to the evaluation of this material. The measurements of carbon monoxide gas sensitivity confirmed that the gas sensing behavior is sensitively dependent on fractal dimensions, fractal densities, and average sizes of the fractal clusters. The random tunneling junction network mechanism was proposed to provide a rational explanation for this gas sensing behavior. The formation process of tin dioxide nanocrystals and fractal clusters could be reasonably described by a novel model.

KEYWORDS: tin dioxide · thin films · fractal strategies · gas-sensing

Semiconductor oxides are fundamental to the development of smart and functional materials, devices, and systems.[1−4] These oxides have two unique structural features: mixed cation valences and an adjustable oxygen deficiency, which are the bases for creating and tuning many novel material properties, from chemical to physical.[5−8] Because of the increasing importance of air pollution and the need to monitor concentration levels of gases such as CO, CO_2, NO_x, O_3, SO_2, *etc.*, the development of many kinds of sensors and control systems has been jolted into action in recent years. Tin dioxide (SnO_2) has been used as a gas sensor material to detect combustible and toxic gases such as CO, NH_3, NO_2, H_2S, and CH_4. Commercial sensors typically use sintered SnO_2 powders, but thin films SnO_2 are gaining increasing popularity.[9,10] With the advent of advanced thin film technology more cost-effective, reproducible devices can be constructed with a reduction in device size and a concomitant increase in the speed of response by using SnO_2 thin films.

It is known that SnO_2 is used as a gas sensor because the number of electrons in the conduction band is affected by the adsorption of gaseous species on its surface.[11] Reducing gas molecules, such as CO, react with the oxygen species (O_2, O_2^-, O^-, and O) on the semiconductor surface.[12] This lowers the height of the Schottky barrier and increases the conductance of the material.[13,14] Gas sensors using SnO_2 are widely used owing to the high sensitivity of SnO_2 to humidity and inflammable gases. In this type of sensors, gas concentration is related to the material's electrical impedance due to the adsorption of gas molecules on the SnO_2 surface. In a pure air environment, SnO_2 adsorbs oxygen that captures its electrons, thereby raising its resistivity. When a reducing gas is present, it competes for the adsorbed oxygen and hence the SnO_2 resistivity decreases. However, the electrical properties of SnO_2 are strongly dependent on material fabrication parameters. Since gas sensing is based on the adsorption mechanisms on the SnO_2 grain surface, for high sensitivity a small grain size is desirable in order to achieve a high specific area, that is, adsorption area per unit volume.[15,16]

The surface conductance of semiconducting oxide is affected by the concentration of ambient gases. Resistive gas sensors are based on this principle and the nature of the sensing mechanism is related to the electrical response of gas sensors to reactive gases. The change in the sensor resistance provides an indication of the gas concentration.[17] These sensors can be quite versatile as they may be used to detect oxygen, flammable gases, and common toxic gases. Their mechanism of operation is complex, involving interactions between gaseous

*Address correspondence to cnzwchen@yahoo.com.cn, mhwu@staff.shu.edu.cn.

Received for review November 17, 2009 and accepted January 12, 2010.

Published online January 19, 2010. 10.1021/nn901635f

molecules and defects on the surface and grain boundaries. The sign of a change in resistance depends on whether the solid has n-type or p-type conductivity.[18,19] Structural properties such as grain size and grain geometry as well as specific surface area can significantly affect the gas sensing properties of semiconducting SnO_2. To control these structural characteristics, the microstructure evolution of SnO_2 thin films should be understood. Fractal method is a potentially powerful technique to characterize microstructures, and we are applying this technique to SnO_2 thin films for the first time in this study. Besides showing some examples of geometric structures of SnO_2 thin films, we shall discuss in detail the applicability and relevance of fractal theory to studying the microstructure and gas sensing behavior of SnO_2-based environmental functional materials.

An integrated device for different gas species is highly desirable for versatile advanced applications. Despite the high sensitivity of SnO_2 to many gases, it is often susceptible to electrical drift which requires long stabilization periods, as well as permanent poisoning after extended periods of operation. New fractal assessment strategies for this material formed at different substrate temperatures are of fundamental importance in the development of microdevices. In this article, we first report on new insight on fractal assessment strategies on SnO_2 thin films prepared by the pulsed laser deposition (*PLD*) technique. We report new results on the experimental preparation of SnO_2 thin films at different substrate temperatures with interesting fractal features. The microstructure evolution of SnO_2 thin films has been investigated using X-ray diffraction and scanning electron microscopy, and its structure has been evaluated by fractal methodology for the first time. The dependence of fractal dimensions on substrate temperature in the SnO_2 thin films has been characterized by fractal theory. Experimental evidence indicated that fractal clusters with various sizes, densities, and fractal dimensions formed in SnO_2 thin films prepared under different substrate temperatures. This formation of significant fractal features is rather unusual. It was found that these fractal structures were sensitively dependent upon the substrate temperature, which was a key parameter affecting the gas sensing behavior. Our findings may enable novel tin dioxide environmental functional materials with appropriate fractal structures to be tailor-made for a large number of applications such as the monitoring of environmental harmful gases and provide new opportunities for future study of fractal structure tin dioxide architectures, with the goal of optimizing environmental functional material properties for specific applications. The complete synthetic experimental details and experimental apparatus is described in detail in Methods.

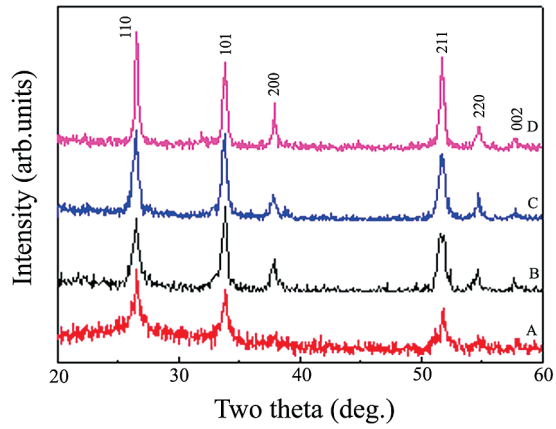

Figure 1. X-ray diffraction (*XRD*) patterns of SnO_2 thin films prepared on Si (100) substrate at temperatures of (A) 300; (B) 350; (C) 400; and (D) 450 °C.

RESULTS AND DISCUSSION

It is known that tin dioxide has a tetragonal rutile crystalline structure (known in its mineral form as cassiterite) with point group D_{4h}^{14} and space group $P4_2/mnm$. The unit cell consists of two metal atoms and four oxygen atoms. Each metal atom is situated amidst six oxygen atoms which approximately form the corners of a regular octahedron. Oxygen atoms are surrounded by three tin atoms which approximate the corners of an equilateral triangle. The lattice parameters are $a = 4.7382(4)$ Å, and $c = 3.1871(1)$ Å. Figure 1 panels A, B, C, and D show X-ray diffraction (XRD) patterns of the SnO_2 thin films prepared on Si (100) substrate at 300, 350, 400, and 450 °C, respectively. The major diffraction peaks of some lattice planes can be indexed to the tetragonal unit cell structure of SnO_2 with lattice constants $a = 4.738$ Å and $c = 3.187$ Å, which are consistent with the standard values for bulk SnO_2 (International Center for Diffraction Data (ICDD), PDF File No. 77-0447). The (*hkl*) peaks observed are (110), (101), (200), (211), (220), and (002). No characteristic peaks belonging to other tin oxide crystals or impurities were detected. The high intensity of these peaks suggests that these thin films mainly consist of the crystalline phase. As the substrate temperature increased, the crystallinity of the thin films was enhanced as manifested by the intensity and sharpness of the XRD peaks of the SnO_2 thin films. The substrate temperature dependence can be interpreted mainly by the mobility of the atoms in the thin films. At low substrate temperatures, the vapor species have a low surface mobility and are located at different positions on the surface. The low mobility of the species will prevent full crystallization of the thin films. However at high substrate temperatures the species with high enough mobility will arrange themselves at suitable positions in the crystalline cell.[23−25] The SnO_2 average grain sizes were calculated using the Scherrer formula: $D = K\lambda/\beta \cos\theta$, where D is the diameter of the nanoparticles, $K = 0.9$, λ (Cu $K\alpha$) = 1.5406 Å, and β is the full-width-at-half-maximum of the diffrac-

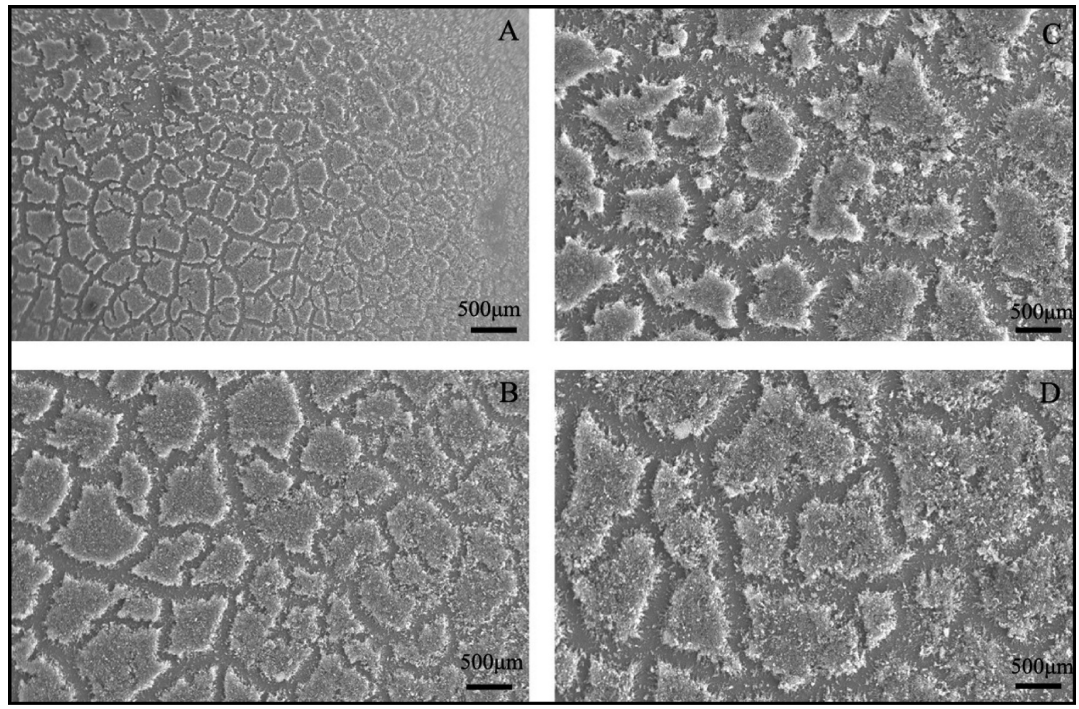

Figure 2. SEM images of SnO_2 thin films prepared on Si (100) substrate at temperatures of (A) 300; (B) 350; (C) 400; and (D) 450 °C.

tion lines. The results show that the average grain sizes of the SnO_2 nanoparticles at different substrate temperatures are in the range of 25.3−27.8 nm. SnO_2 nanoparticle size increases from 25.3 nm at 300 °C to 26.2 nm at 350 °C. It then increases to 27.0 nm at 400 °C and finally to 27.8 nm at 450 °C. In fact, SnO_2 nanostructures can work as sensitive and selective chemical sensors. SnO_2 nanostructure sensor elements can be configured as resistors whose conductance can be modulated by charge transfer across the surface or as a barrier junction device whose properties can be controlled by applying a potential across the junction. Functionalizing the surface further offers a possibility to improve their sensing ability based on a better understanding of the influence of significant microstructural features, for example, the development of gas sensors for the detection of environmentally harmful gases.

Figure 2 presents scanning electron microscopy (SEM) images of SnO_2 thin films prepared on Si (100) substrate at temperatures of (A) 300, (B) 350, (C) 400, and (D) 450 °C, respectively. The SEM observation indicated that all thin films produced under different substrate temperatures exhibited self-similar fractal patterns. It can be seen from Figure 2 that the fractal patterns are open and loose structure with increasing substrate temperature. The average sizes of the fractal patterns (or clusters) are about 0.307 μm (see Figure 2A), 0.906 μm (see Figure 2B), 1.202 μm (see Figure 2C), and 1.608 μm (see Figure 2D). The average sizes of the fractal clusters for four thin films were estimated by

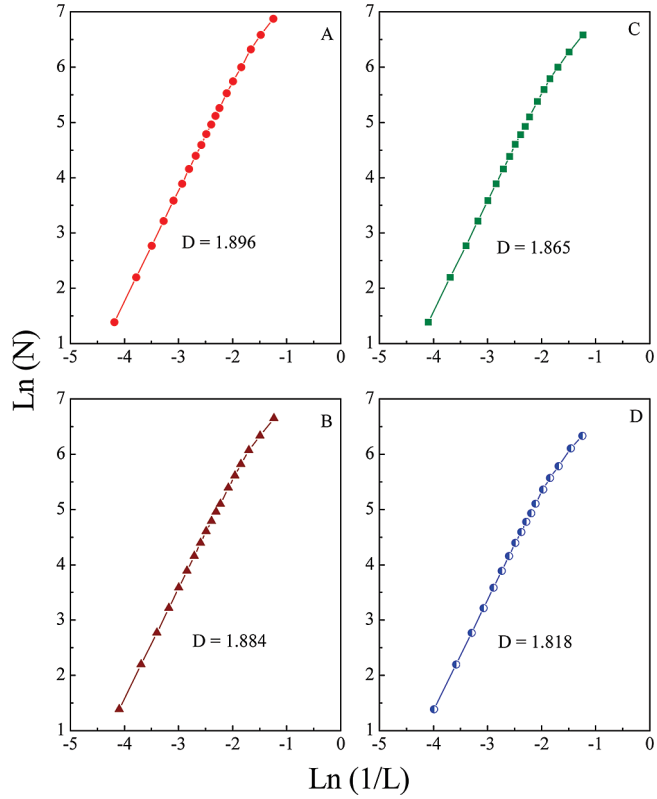

Figure 3. Plots of ln(*N*) *versus* ln(1/*L*) of the fractal cluster regions in Figure 2, where *L* is the box size and *N* is the number of boxes occupied by the SnO_2 crystalline structure for substrate temperatures at (A) 300; (B) 350; (C) 400; and (D) 450 °C.

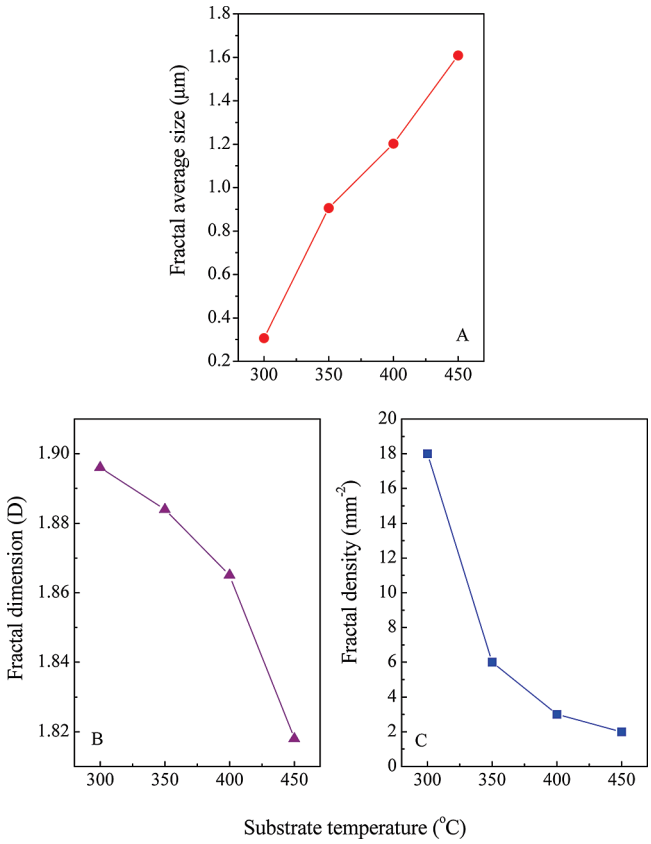

Figure 4. (A) The fractal average size; (B) the fractal dimension; (C) the fractal density *versus* the substrate temperature.

measurement on the fractal regions. The measuring procedure is as follows: for each SEM image, we chose 10 fractal patterns at random to get an average value. The average sizes of the fractal patterns were obtained by averaging the values of SEM images with different orientations. It was found that the average sizes of the fractal clusters increase with increasing substrate temperature.

Figure 3 shows that the plots of ln(*N*) *versus* ln(1/*L*) of the fractal cluster regions in Figure 2, where *L* is the box size and *N* is the number of boxes occupied by the SnO_2 clusters. It can be seen that all plots show good linearity, which means that the morphologies of SnO_2 clusters have scale invariance within these ranges. So the SnO_2 clusters can be regarded as fractals. To obtain the fractal dimension (*D*), we fit a linear relationship for the function ln(*N*) *versus* ln(1/*L*). The results show that the fractal dimension (*D*) is 1.896 at 300 °C as shown in Figure 3A, 1.884 at 350 °C as shown in Figure 3B, 1.865 at 400 °C as shown in Figure 3C, and 1.818 at 450 °C as shown in Figure 3D. We found that the fractal dimension (*D*) decreases with increasing substrate temperature. The smaller fractal dimension means that the SnO_2 thin films are composed of the open and loose fractal structure with finer branches. Figure 4 panels A−C show the distribution of the fractal average size, fractal dimension, and fractal density for different substrate temperatures. It can be seen that there is an obvious increase in average fractal size (see Figure 4A), and the fractal dimension generally decreases (see Figure 4B) with increasing substrate temperature. In general, the fractal density is determined by the initial nucleation probability of the core crystal. From Figure 4C, the fractal density was calculated to be 18, 6, 3, and 2 mm^{-2} at 300, 350, 400, and 450 °C, respectively. It was found that the fractal density gradually decreases with increasing substrate temperature. In the present work, the initial increase in nucleation probability was due to strain relaxation caused by the low short-range temperature field at 300 °C, so that the fractal density and their occupation area were high. With the increase of substrate temperature, the higher long-range temperature field may promote new nuclei and subsequent growth, which leads to the fractal growth of the fine branches and a lower fractal density. This fractal structure may lead to improvement in the design of gas sensors for the monitoring of environmental pollutants.

On the basis of our experimental observation, the formation process of SnO_2 nanocrystals and fractal clusters could be reasonably described by a novel model and be separated into eight steps, which are illustrated in detail in Figure 5.

(i) Operation of the KrF excimer laser at a repetition rate of 10 Hz at an incident angle of 45° to the pol-

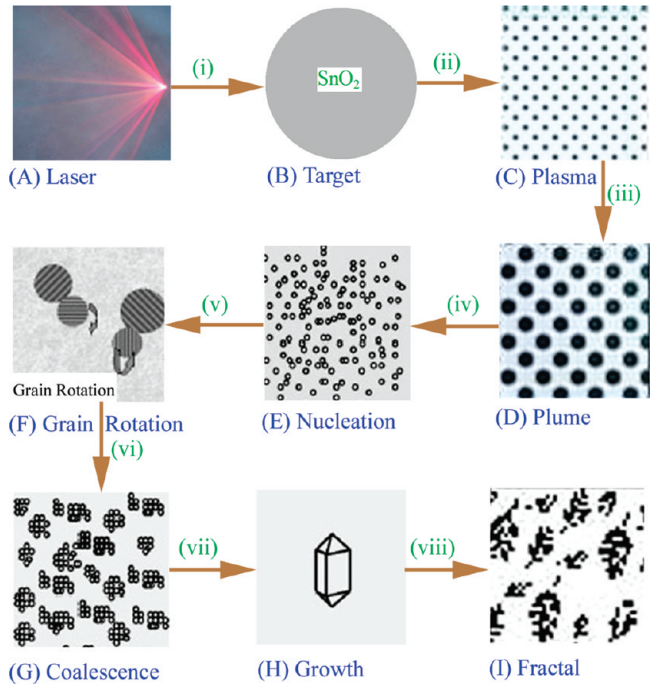

Figure 5. The formation process of SnO_2 nanocrystals and fractal clusters: (A) laser; (B) target; (C) plasma; (D) plume; (E) nucleation; (F) grain rotation; (G) coalescence; (H) growth; and (I) fractal.

ished sintered cassiterite SnO_2 target rotating at a rate of 15 rpm to avoid drilling.

(ii) Production of the high-temperature and high-pressure tin dioxide plasma at the solid−liquid interface quickly after the interaction between the pulsed laser and SnO_2 target.

(iii) Subsequent expansion of the high-temperature and high-pressure tin dioxide plasma leading to cooling of the tin dioxide plumes.[26−29] In our case, the interval between two successive pulses is much longer than the life of the plasma. Therefore, the next laser pulse had no interaction with the former plasma.

(iv) Deposition of the tin dioxide plume on the Si (100) substrate after the disappearance of the plasma, inducing the initial nucleation of SnO_2 nanocrystals.

(v) Grain rotation culminating in a low-energy configuration. This process is directly related to the reduction of surface energy, aimed at minimizing the area of high-energy interfaces.[30,31]

(vi) Possible formation of a coherent boundary between grains due to grain rotation, with the consequence of removing the common grain boundary and culminating in a single larger SnO_2 nanocrystal. This is the coalescence process.

(vii) Growth of SnO_2 nanocrystals along preferred crystallographic directions which could be predicted by an analysis of the surface energy in several crystallographic orientations.

(viii) Formation of the fractal structure as SnO_2 crystallizes and nucleates at high energy interfaces such as grains boundaries.

According to the fractal theory,[32,33] the heat released by crystallization leads to a local temperature rise in the surrounding area and this temperature field can propagate quickly and stimulate new nuclei appearing randomly in nearby regions. The stimulated nuclei of the next generation can also cause a local temperature rise and repeat the above process many times until SnO_2 fractal patterns are formed. On the basis of the above proposed formation mechanism, we characterize the formation processes of SnO_2 nanocrystals and fractal structure in Figure 5A−I. We believe that laser ablation technique is an appropriate method to synthesize a series of environmental functional materials with controlled composition, morphology, and nanocrystal size, which are important in the study of the sensitivity of SnO_2 thin films.

To verify the gas sensing behavior of these SnO_2 thin films with interesting features of the fractal structure, we investigate the sensitivity dependence on carbon monoxide (CO) concentration, so as to achieve the aim of monitoring environmental pollutants. Figure 6 shows the CO gas sensing behavior of the SnO_2 thin films prepared on Si (100) substrate at (A) 300, (B) 350, (C) 400, and (D) 450 °C, respectively. The measurement was performed at room temperature with CO concentrations of 25, 50, 75, 100, 200, 300, 400, and 500 ppm. We observe that the sensitivity increases with increasing CO concentration and substrate temperature. Similarly Cooper and Cicera found their SnO_2 thin film sensor possessed higher sensitivity to CO by using different procedures.[34,35] Further advancement of this gas sensor fabricated by the SnO_2 thin films with fractal structure to detect environmental harmful gases such as CO requires a clear understanding of its gas sensing mechanism. Our experimental results show that the CO gas sensing behavior clearly depends on the fractal dimension, fractal density, and average sizes of the fractal clusters (see Figures 4 and 6). We propose a random tunneling junction network (RTJN) mechanism to explain this gas sensing behavior. After the fractal formation, the fractal clusters consist of the SnO_2 grains with the morphology of fine dendrite-like nanocrystals incorporating many tunneling junctions of varying sizes. From the view of electron transport, the whole thin film is made up of a series of tunneling junctions. For the SnO_2 thin films deposited at different substrate temperatures, the sizes of the fractal branches with different fractal dimensions are different, leading to differences in the height of the Schottky barrier of the tunneling junctions, with the consequence that the breakdown voltages are also different. During the measurement of the gas sensitivity, the reducing gas molecules such as CO react with the oxygen species (O_2, O_2^-, O^-, and O) ionized on the surface of the SnO_2 particles. This lowers the height of the Schottky barrier, and increases the conductance.[12−14] For example, for the SnO_2 thin film deposited at the lower substrate temperature (*e.g.*, at 300 °C) with the larger fractal dimension, the junction *i* will have the higher resistance state due to the thicker fractal branches, so the external voltage V_i cannot lower the Schottky barrier S_i and the junction *i* cannot be broken. The gas sensitivity is then lowered (see Figure 6A). Conversely, for the SnO_2 thin film deposited at the higher substrate temperature (*e.g.*, at 450 °C) with the smaller fractal di-

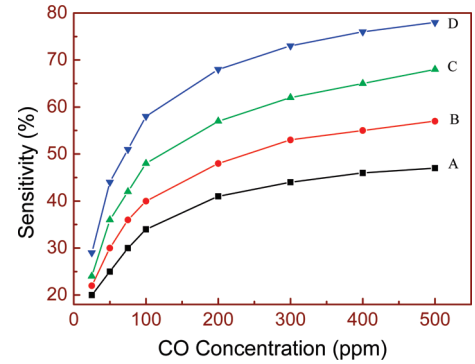

Figure 6. The CO gas sensing behavior of SnO_2 thin films prepared on Si (100) substrate at temperatures of (A) 300; (B) 350; (C) 400; and (D) 450 °C.

mension, the junction *i* will have the lower resistance state due to the finer fractal branches, so the external voltage V_i can lower the Schottky barrier S_i and the junction *i* will be broken. Therefore, the gas sensitivity would be higher (see Figure 6D). As mentioned above, there is a relationship between the fractal dimension and the size of the fractal branches in that the number of the fine branches increases with decreasing fractal dimension. Therefore, the smaller the fractal dimension, the larger the number of junctions with the smaller Schottky barrier S_i and lower resistance state. The present findings reveal new opportunities for future study of fractal structure tin dioxide architectures, with the goal of optimizing environmental functional material properties for specific applications.

CONCLUSION

We have prepared SnO_2 thin films at different substrate temperatures with interesting fractal features. The experimental evidence indicated that the fractal clusters with various sizes, densities, and fractal dimensions were affected by different substrate temperatures. This formation of significant fractal features is rather unusual. This process could be reasonably described by a novel model: (i) operation of the KrF excimer laser; (ii) production of the tin dioxide plasma; (iii) cooling of the tin dioxide plumes; (iv) deposition of the tin dioxide plume on the Si substrate; (v) grain rotation; (vi) formation of coherent boundary between grains followed by coalescence; (vii) growth of SnO_2 nanocrystals along preferred crystallographic directions; and (viii) formation of the fractal structure. CO gas sensitivity measurement confirmed that the gas sensing behavior is sensitively dependent on fractal dimensions, fractal densities, and average sizes of the fractal clusters. It was found that the sensitivity increases with increasing CO concentration and decreasing fractal dimension. We have shown that fractal methodology can be applied to the evaluation of tin dioxide thin films. This gas sensing behavior could be explained by the random tunneling junction network (RTJN) mechanism.

METHODS

To obtain the sintered SnO_2 target for pulsed laser deposition (PLD), we synthesized a pure nanocrystalline SnO_2 powder by the sol−gel method.[20] The fabrication method is described in the following. Meta-stannic acid sol (parent sol) was precipitated by treating a cold ethanol solution of $SnCl_4$ (27%) with an aqueous ammonia solution (28%) until a suitable pH value was reached. Dry powder with average grain size of about 4 nm was obtained by drying the parent sol, which had been washed repeatedly with deionized water. The SnO_2 discs, 15 mm in diameter and 4 mm in thickness, were prepared by compacting the powder under uniaxial pressure of 0.4 GPa, and sintered at 1150 °C for 2 h. The sintered disk consisted of high-purity cassiterite structure SnO_2 (99.8%).

SnO_2 thin film was prepared by PLD techniques using the above sintered SnO_2 disk[3]. The target was cleaned with methanol in an ultrasonic cleaner before installation to minimize contamination. The laser was a KrF excimer laser (Lambda Physik, LEXtra 200, Germany) producing pulse energies of 350 mJ at a wavelength of 248 nm and a frequency of 10 Hz. The duration of every excimer laser pulse was 34 ns. The laser energy was transmitted onto the target in a high-vacuum chamber through a UV-grade fused silica window using an UV-grade fused silica lens. During the experiment, the target was kept rotating at a rate of 15 rpm to avoid drilling. The fluence was set at 5 J/cm^2 per pulse, corresponding to a total of approximately 1.5×10^5 laser pulses. The growth rate was estimated to be about 0.3 nm/s (or about 1 μm/h). The ablated substance was collected on a Si (100) substrate mounted on a substrate holder 4 cm away from the target. The high vacuum in the deposition chamber was achieved by using a cryopump (Edwards Coolstar 800). The base pressure prior to laser ablation was about 1×10^{-6} mbar, and the oxygen partial pressure during laser ablation was set about 3×10^{-2} Pa. All deposition processes were carried out by *in situ* operation on the substrate at temperatures of 300, 350, 400, and 450 °C.

X-ray diffraction (XRD) was performed with a Philips X'pert diffractometer using Cu Kα radiation (1.5406 Å) in reflection geometry. A proportional counter with an operating voltage of 40 kV and a current of 40 mA was used. XRD patterns were recorded at a scanning rate of 0.05° s^{-1} in the 2θ ranges from 20° to 60°. Scanning electron micrographs were obtained using a JEOL-JSM6335F scanning electron microscope (SEM). SEM images were digitized by using the Fractal Images Process Software (FIPS). These digitized images were divided into boxes of 360 × 360 size and then processed by the fractal theory.[21] Four intact fractal patterns were selected from these digitized images. The average value of the fractal dimensions (*D*), the fractal density and the average size of the fractal clusters for these digitized fractal patterns were obtained by using the box-counting method.[22] The carbon monoxide (CO) gas sensing property in the sensor was measured by a simple electrical measuring system. The test CO gas was introduced in the chamber by an injector with variable volume which facilitated control of gas concentration in the range 25−500 ppm. After the sensor was stabilized, the process was repeated by injecting a higher amount of the CO gas.

Acknowledgment. The work described in this article was financially supported by the National Natural Science Foundation of China (40830744 and 20871081), the Special Funds for Major State Basic Research Projects of China (973 Program: 2006CB705604), the National Major Project of Science & Technology Ministry of China (2008ZX07421-004), the Shanghai Leading Academic Discipline (S30109), the Shanghai Key Program (08520512200, 09530501200, and 09XD1401800), and the Innovation Funds of Shanghai Municipal Education Commission (SHMEC, 10ZZ64) and Shanghai University. This work also was supported by a grant from the Research Grants Council of the Hong Kong Special Administrative Region, China (Project No. CityU 1228/08P).

REFERENCES AND NOTES

1. Wang, Z. L.; Kang, Z. C. *Functional and Smart Materials-Structural Evolution and Structure Analysis;* Plenum Press: New York, 1998.
2. Pan, Z. W.; Dai, Z. R.; Wang, Z. L. Nanobelts of Semiconducting Oxides. *Science* **2001**, *291*, 1947–1749.
3. Chen, Z. W.; Lai, J. K. L.; Shek, C. H. Insights into Microstructural Evolution from Nanocrystalline SnO_2 Thin Films Prepared by Pulsed Laser Deposition. *Phys. Rev. B* **2004**, *70*, 165314-1–165314-7.
4. Chen, Z. W.; Lai, J. K. L.; Shek, C. H. Quantum dot formation and dynamic scaling behavior of SnO_2 nanocrystals

induced by pulsed delivery. *Appl. Phys. Lett.* **2006**, *88*, 033115-1–033115-4.
5. Dai, Z. R.; Gole, J. L.; Stout, J. D.; Wang, Z. L. Tin Oxide Nanowires, Nanoribbons, and Nanotubes. *J. Phys. Chem. B* **2002**, *106*, 1274–1279.
6. Wang, Z. L. Nanobelts, Nanowires, and Nanodiskettes of Semiconducting Oxides—From Materials to Nanodevices. *Adv. Mater.* **2003**, *15*, 432–436.
7. Ng, H. T.; Li, J.; Smith, M. K.; Nguyen, P.; Cassell, A.; Han, J.; Meyyappan, M. Growth of Epitaxial Nanowires at the Junctions of Nanowalls. *Science* **2003**, *300*, 1249.
8. Cheng, B.; Russell, J. M.; Shi, W. S.; Zhang, L.; Samulski, E. T. Large-Scale, Solution-Phase Growth of Single-Crystalline SnO_2 Nanorods. *J. Am. Chem. Soc.* **2004**, *126*, 5972–5973.
9. Mikko, U.; Hanna, L.; Heli, V.; Lauri, N.; Resch, R.; Gernot, F. Atomic force microscopy studies of SnO_2 Thin Film Microstructures Deposited by Atomic Layer Epitaxy. *Mikrochim. Acta* **2000**, *133*, 119–123.
10. Hidalgo Falla, P.; Peres, H. E. M.; Gouvêa, D.; Ramirez-Fernandez, F. J. Doped Tin Oxide Nanometric Films for Environment Monitoring. *Mater. Sci. Forum* **2005**, *498−499*, 636–641.
11. Oyabu, T. Sensing Characteristics of SnO_2 Thin Film Gas Sensor. *J. Appl. Phys.* **1982**, *53*, 2785–2787.
12. Chen, Z. W.; Lai, J. K. L.; Shek, C. H. Facile Strategy and Mechanism for Orthorhombic SnO_2 Thin Films. *Appl. Phys. Lett.* **2006**, *89*, 231902−1231902−3.
13. Demarne, V.; Grisel, A. An Integrated Low-Powder Thin Film CO Gas Sensor on Silicon. *Sens. Actuators* **1988**, *13*, 301–313.
14. Dos Santos, O.; Weiller, M. L.; Junior, D. Q.; Medina, A. N. CO Gas-Sensing Characteristics of SnO_2 Ceramics Obtained by Chemical Precipitation and Freeze-Drying. *Sens. Actuta. B* **2001**, *75*, 83–87.
15. Shukla, S.; Seal, S.; Ludwing, L.; Parish, C. Nanocrystalline Indium Oxide-Doped Tin Oxide Thin Film As Low Temperature Hydrogen Sensor. *Sens. Actutators, B* **2004**, *97*, 256–265.
16. Harbeck, S.; Szatvanyi, A.; Barsan, N.; Weimar, U.; Hoffmann, V. Drift Studies of Thick Film Un-Doped and Pd-Doped SnO_2 Sensors: Temperature Changes Effect and CO Detection Mechanism in the Presence of Water Vapour. *Thin Solid Films* **2003**, *436*, 76–83.
17. Windischmann, H.; Mark, P. A Model for the Operation of a Thin-Film SnO_x Conductance-Modulation Carbon Monoxide Sensor. *J. Electrochem. Soc.* **1979**, *126*, 627–633.
18. Lantto, V.; Romppainen, P. Electrical Studies on the Reactions of CO with Different Oxygen Species on SnO_2 Surface. *Surf. Sci.* **1987**, *192*, 243–264.
19. Romppainen, P.; Lantto, V. The Effect of Microstructure on the Height of Potential Energy Barriers in Porous Tin Dioxide Gas Sensors. *J. Appl. Phys.* **1988**, *63*, 5159–5165.
20. Shek, C. H.; Lai, J. K. L.; Lin, G. M. Investigation of Interface Defects in Nanocrystalline SnO_2 by Positron Annihilation. *J. Phys. Chem. Solids* **1999**, *60*, 189–193.
21. Chen, Z. W.; Zhang, S. Y.; Tan, S.; Hou, J. G.; Zhang, Y. H. Fractal Formation and Tunneling Effects on the Conductivity of Au/a-Ge Bilayer Films. *Thin Solid Films* **1998**, *322*, 194–197.
22. Feder, J. *Fractal;* Plenum Press: New York, 1988; 15.
23. Fallah, H. R.; Ghasemi, M.; Hassanzadeh, A. Influence of Heat Treatment on Structural, Electrical, Impedance and Optical Properties of Nanocrystalline ITO Films Grown on Glass at Room Temperature Prepared by Electron Beam Evaporation. *Phys. E* **2007**, *39*, 69–74.
24. Chen, Z. W.; Lai, J. K. L.; Shek, C. H.; Chen, H. D. Nucleation and Growth of SnO_2 Nanocrystallites Prepared by Pulsed Laser Deposition. *Appl. Phys. A* **2005**, *81*, 959–962.
25. Kim, Y. J.; Kim, Y. T.; Yang, H. K.; Park, J. C.; Han, J. I.; Lee, Y. E.; Kim, H. J. Epitaxial Growth of ZnO Thin Films on R-Plane Sapphire Substrate by Radio Frequency Magnetron. *J. Vac. Sci. Technol. A* **1997**, *15*, 1103–1107.
26. Zhu, S.; Lu, Y. F.; Hong, M. H.; Chen, X. Y. Laser Ablation of Solid Substrates in Water and Ambient Air. *J. Appl. Phys.* **2001**, *89*, 2400–2403.
27. Kim, D.; Lee, H. Enhanced Ablation and Photoacoustic Excitation in near-Threshold Laser Ablation of Liquid-Coated Surfaces. *J. Appl. Phys.* **2001**, *89*, 5703–5706.
28. Zhu, S.; Lu, Y. F.; Hong, M. H. Laser Ablation of Solid Substrates in a Water-Confined Environment. *Appl. Phys. Lett.* **2001**, *79*, 1396–1398.
29. Berthe, L.; Fabbro, R.; Peyre, P.; Tollier, L.; Bartnicki, E. Shock Waves from a Water-Confined Laser-Generated Plasma. *J. Appl. Phys.* **1997**, *82*, 2826–2832.
30. Penn, R. L.; Banfield, J. F. Morphology Development and Crystal Growth in Nanocrystalline Aggregates under Hydrothermal Conditions: Insights from Titania. *Geochim. Cosmochim. Acta* **1999**, *63*, 1549–1557.
31. Penn, R. L.; Banfield, J. F. Imperfect Oriented Attachment: Dislocation Generation in Defect-Free Nanocrystals. *Science* **1998**, *281*, 969–971.
32. Hou, J. G.; Wu, Z. Q. Temperature Dependence of Fractal Formation in Ion-Implanted α-Ge/Au Bilayer Thin Films. *Phys. Rev. B* **1989**, *40*, 1008–1012.
33. Chen, Z. W.; Zhang, S. Y.; Tan, S.; Hou, J. G.; Zhang, Y. H. Effect of Fractal Crystallization on the Depositing Sequence of a Pd/Ge Thin Film System. *J. Vac. Sci. Technol. A* **1998**, *16*, 2292–2294.
34. Cooper, R. B.; Advani, G. N.; Jordan, A. G. Gas Sensing Mechanisms in SnO_2 Thin Films. *J. Electron. Mater.* **1981**, *10*, 455–472.
35. Cicera, A.; Dieguez, A.; Diaz, R.; Cornet, A.; Morante, J. R. New Method to Obtain Stable Small-Sized SnO_2 Powders for Gas Sensors. *Sens. Actuators, B* **1999**, *58*, 360–364.